Title

Electrochemical performance of Si/CeO2/Polyaniline composites as anode materials for lithium ion batteries

Authors

Bai, Ying
Tang, Yang
Wang, Zhihui
et al.

Publication Date

2015-04-01

DOI

10.1016/j.ssi.2014.12.016

Peer reviewed

Electrochemical performance of Si/CeO_2/Polyaniline as anode materials for lithium-ion battery

Ying Bai[a], Yang Tang[a], Chuan Wu[*a], Feng Wu[a], Gao Liu[*a]

[a] School of Chemical Engineering & Environment, Beijing Institute of Technology, Beijing 100081, China

[b] Environmental Energy Technologies Division, Lawrence Berkeley National Laboratory, Berkeley, California 94720, United States

Correspondence: chuanwu@bit.edu.cn (C. Wu), gliu@lbl.gov (G. Liu)

Abstract

Si has very high theoretical specific capacity as an anode material in a lithium-ion battery. However, its application is seriously restricted because of relatively undesirable conductivity and poor cycling stability. Here we report Si/CeO_2/Polyaniline (SCP) composites which were synthesized by hydrothermal reaction and chemical polymerization. The structures and morphologies of the SCP composites are confirmed by X-ray diffraction (XRD), scanning electronic microscopy (SEM) and transmission electron microscopy (TEM). It is shown that Si/CeO_2 (SC) particles are well coated by PANI elastomer with good conductivity. The SCP displays larger reversible capacities and better cycling performance compared with pure Si because CeO_2 can protect Si from reacting with electrolyte. What's more, the PANI elastomer can accommodate the volume change of the

composite during Li-alloying/dealloying processes, so the pulverization of silicon would be well inhibited. The SCP material can retain a capacity nearly 775 mAh/g after 100 cycles, while pure Si only keeps 370mAh/g after 100 cycles.

1. Introduction

Lithium ion batteries have been widely used in the world now, and graphite is common commercial anode material because it's cheap and exhibits perfect cycling performance. However, graphite's theoretical specific capacity is only about 370 mAh/g, which limits the improvement of LIBs[1]. Therefore, it's necessary to find new anode materials with high specific capacities. Si is drawn much attention as an anode material for LIBs because of high theoretical specific capacity (nearly 4200 mAh/g). But its application is seriously restricted due to relatively undesirable conductivity and poor cycling stability which is attributed to significant volume change during lithiation and delithiation processes. To overcome the problems, many researchers adopt lots of methods such as Si-C[2-12], Si-metal[13-20] and Si with special structure (core–shell[21-23], porous[24, 25], nanotube[26], nanowire[27], film[28]). In Si-C and Si-metal composites above-mentioned, the C and metal can enhance the conductivity and buffer the mechanical stress caused by volume change of Si as a matrix; and the special structure also provide enough space to accommodate the expansion of Si.

Here in this work, we report a Si/CeO_2/polyaniline (SCP) composite as anode material for LIBs which is synthesized through hydrothermal reaction and chemical

polymerization. CeO_2 can enable to improve the coulombic efficiency as a protect layer between Si and electrolyte. And the PANI elastomer can buffer the mechanical stress caused by Si to keep the structure steady.

2. Experimental

The SCP material was synthesized through hydrothermal reaction and chemical polymerization.

First, it's the hydrothermal reaction. Cerium nitrate (Ce $(NO_3)_3 \cdot 6H_20$), crystalline silicon nanopowder (Si, 20-50nm, 97%, Strem Chemicals) and cetyl trimethyl ammonium bromide (CTAB) were dissolved in a mixture of distilled water and alcohol (volume ratio of 1:1). The mixture was transferred into a stainless steel autoclave, and keeped at 180℃ for 12h, then cooled to room temperature. The product was centrifuged, washed and dried under vacuum at 60℃ for 20h to get Si/CeO_2 (SC). The mole ratio of Ce were 0%, 0.1%, 0.5%, 1% and 2%, which were marked as SC00, SC01, SC05, SC10 and SC20.

After SC particles were got, the chemical polymerization can be carried out to prepare SCP. 1.24g dodecyl benzenesulfonic acid (ABS) was added into 50mL distilled water and stired for 4h to get a homogeneous microemulsion. Then 0.24g aniline was mixed with the homogeneous microemulsion by keeping stirring for 4h. Afterwards, 0.56g SC particles were added into the mixture with ultrasonication for 1h. The mixture was subsequently stirred for 30min, and then 0.56g ammonium persulphate (APS, 0.5M) was added into it. Maintaining stirring for 24h, emerald

powder of SCP was obtained after centrifuging, washing and drying in vacuum at 60℃ for 24h. With the mole ratio changing in SC particles, the SCP materials were marked as SCP00, SCP01, SCP05, SCP10 and SCP20.

The structures and morphologies of materials were analyzed by X-ray diffraction (XRD, Rigaku Ultima IV-185), scanning electronic microscopy (SEM, QUANTA FEG 250) and transmission electron microscopy (TEM, FEI Tecnai G2 F30).

The electrochemical performance was tested using coin cells. The work electrode was prepared by mixing the active materials, super-p and poly (vinylidene fluoride) (PVDF) binder with a mass ratio of 8:1:1 to form homogeneous slurry. The slurry was coated on a copper foil, and then dried at 80℃ for 12 h.

Coin cell was assembled in a glove box full of argon, while the counter electrode was lithium metal and the electrolyte was 1 M $LiPF_6$ solution in a mixture of ethylene carbonate (EC), ethyl methyl carbonate (EMC) and diethyl carbonate (DEC) (volume ratio of 1:1:1). And the membrane was Celgard 2400 polypropylene membrane.

The cells were galvanostatically charged and discharged at 100 mA/g in the voltage range of 0~2V (vs. Li^+/Li). Cyclic voltammetry (CV, ChI660d) was carried out under a sweep speed of 0.1mV/s between 0.01V and 2V (vs. Li^+/Li). All measurements were carried out at room temperature.

3. Results and discussion

3.1. Physical characterization

The XRD patterns of SCP materials are shown in Fig. 1. The peaks

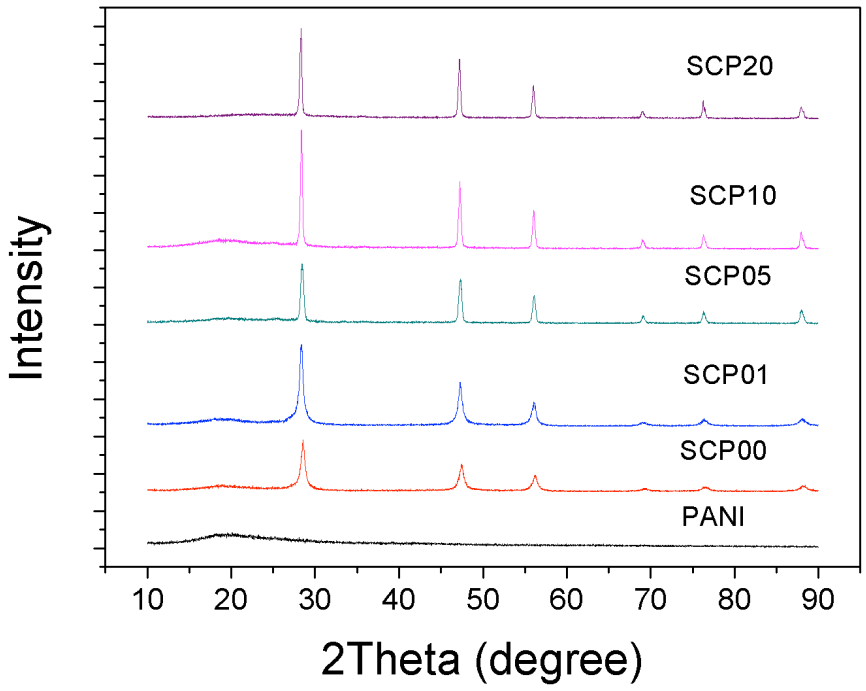

Fig. 1 XRD patterns of PANI and SCP

near 2Theta=28, 47, 56, 69, 76 and 88 indicate the crystalline structure of Si, which doesn't change after the addition of CeO_2 and PANI, as no other peaks are observed. It also can be seen that PANI has a wide peak near 2Theta=22, and the peak also exists in other plots. It indicates the SCP materials actually contain PANI. As shown in Table 1, the lattice constant and unit cell volume of SCP increase a

Table 1 The lattice constant and unit cell volume of SCP

SCP	lattice constant(Å)	unit cell volume(Å)^3
SCP00	5.42053	159.27
SCP01	5.43301	160.37
SCP05	5.43599	160.63
SCP10	5.43707	160.73
SCP20	5.43821	160.83

little with increasing content of Ce. That means more space for lithiation and delithiation which can improve the reversible capacity[29].

Fig. 2 shows the SEM images of Si (a), SC05 (b) and SCP05 (c). Three kinds of nano-size particles' average diameters are all about 50 nm, which indicates larger specific surface area. The additions of CeO_2 and PANI slightly affect the particles' morphologies. As shown in Fig. 2b, the SC particles seem a little larger than Si particles, while slight agglomeration can be observed because of the high stress in reaction. The boundary among particles become indistinct after PANI coating (Fig. 2c), because the PANI layer covers on the surface

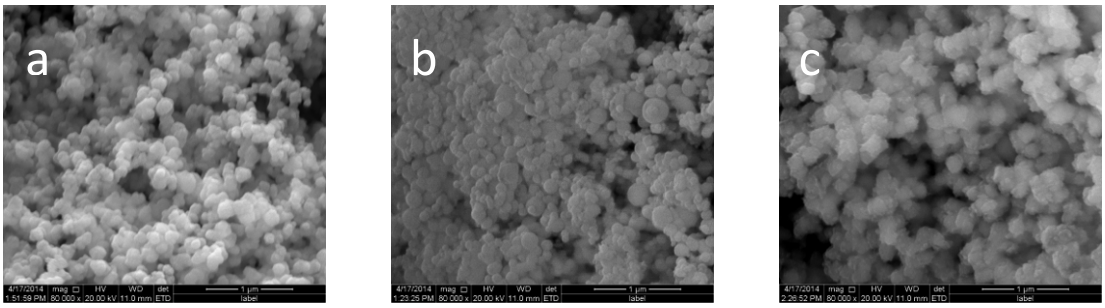

Fig. 2 SEM images of Si (a), SC05 (b) and SCP05 (c)

of the particles so that the particles are connected by the PANI layer.

Fig. 3 shows TEM images of Si (a, f), SC05 (b, d, g) and SCP05 (c, e, h). It can be seen that the nanoparticles distribute well (Fig. 3a, b, c, with the same magnification of 80000) and the diameters of most

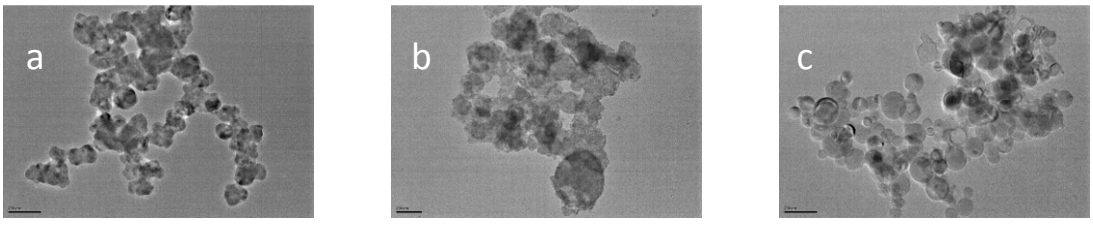

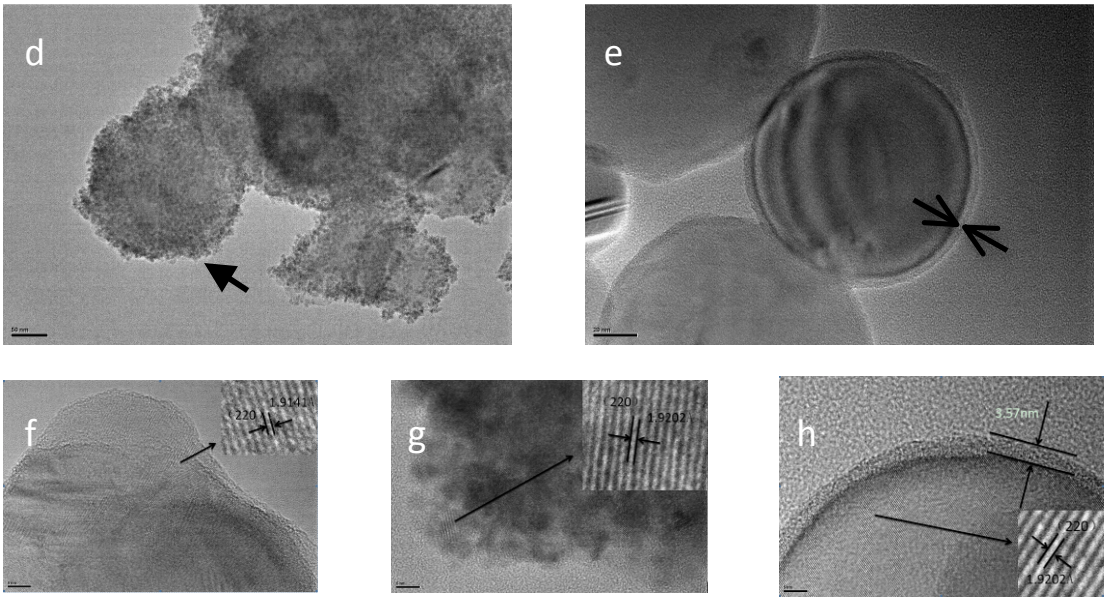

Fig. 3 TEM images of Si (a, f), SC05 (b, d, g) and SCP05 (c, e, h)

particles are about 50nm. While we observe that some CeO_2 particles adhere to the Si particles' surface (Fig. 3d) and the PANI coating on the surface of SC particle can be easily distinguished (Fig. 3e, the layer between two arrows). After the addition of CeO_2, the interplanar spacing of (220) plane increases from 1.9141Å to 1.9202Å (Fig. 3f, g), which indicates that the lattice constant also develop, while the interplanar spacing of (220) plane keeps 1.9202Å (Fig. 3h) with the coverage of PANI (3.57nm), as well as the lattice constant don't change.

3.2. Electrochemical performance

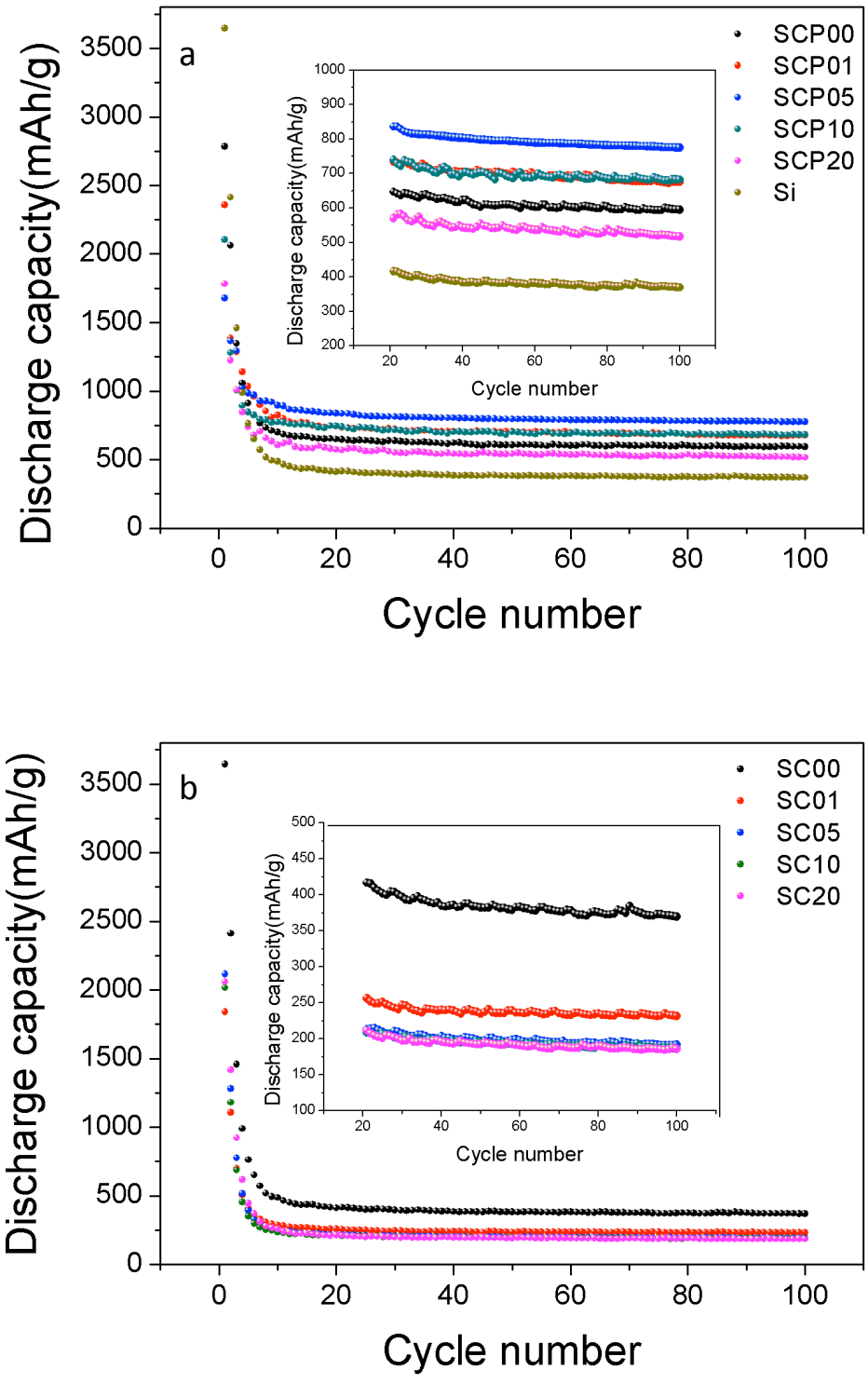

Fig. 4 Cycling performance of (a) SCP, Si and (b) SC

Fig. 4a shows the cycling performance of SCP materials with different cerium content and pure Si. As we see, the initial capacities of SCP00, SCP01, SCP05,

SCP10 SCP20 and Si are 2783.4, 2357, 1678.6, 2104.7, 1783.4 and 3645.5 mAh/g, respectively. After 10 cycles, the capacities decrease to 699.9, 823.8, 895, 774.3, 607.4 and 487mAh/g. After the volume changes during lithiation and delithiation processes in the first ten cycles, the capacities become steady relatively. At the 20th cycle, the capacities of SCP00, SCP01, SCP05, SCP10, SCP20 and Si are 649.2, 741.3, 837.5, 743.5, 574 and 411.8mAh/g, respectively. SCP00, SCP01, SCP05, SCP10, SCP20 and Si retain capacities of 594.8, 675.3, 774.8, 682.5, 517.1 and 369.4mAh/g after 100 cycles. With increasing amount of cerium, the cycling performances of SCP samples tend to be better. Especially for SCP05 sample, after 100 cycles the capacity still retains nearly 775mAh/g, which is higher than those of other SCP samples and Si (369.4mAh/g). The phenomenon may be attributed to that CeO_2 can prevent the SCP material from directly contacting with the electrolyte as a protective layer to restrain the reactions between them, so the cycling reversibility is promoted. However, when the amount of cerium is more than 0.5%, the reversible capacity after 10th cycle begins to descend, as CeO_2 is not electrochemistry-active and the reversible capacity of SCP will dramatically decrease with excessive CeO_2. Therefore, the SCP05 displays larger reversible capacities and better cycling performance compared with other SCP materials.

The effect of PANI to SCP is shown in Fig. 4b. Without PANI compared with SCP, all the SC samples except SC00 exhibit lower discharge capacity than pure Si (SC00) sample, because the huge volume change cannot be well inhibited so that pulverization of particles and destruction of structure occur. PANI is like elastomer

which effectively buffers the huge volume change of Si during lithiation and delithiation processes via providing enough room for the expansion. At the same time, the PANI also improves the conductivities of SCP composites. In consideration of the important effect of PANI, then we'll focus on the electrochemical performance of Si and SCP samples.

Fig. 5a shows the initial discharge-charge curves of Si, SCP00 and SCP05 at the current density of 100mA/g. The initial discharge capacities of Si, SCP00 and SCP05 are 3645.5, 2783.4 and 1678.6 mAh/g, while their initial charge capacities are 2453.4, 2135.1 and 1471.2 mAh/g, respectively. The irreversible capacity is caused by the formation of SEI film and lithium ion caught in the crystal. The coulombic efficiencies of the PANI modified samples are improved with increasing PANI content, namely, 76.7% for SCP00 and 87.6% for SCP05, which are much superior to that of pure Si, 67.3%. It indicates that PANI buffers the volume expansion to prevent the pulverization of Si and CeO_2, as well as suppresses the side reactions between Si and electrolyte, which are both beneficial to improving the reversible capacity. It can be seen that the profiles of SCP00 and SCP05 are similar to that of Si, indicating that the existence of CeO_2 and PANI does not change the lithiation and delithiation behaviors. During the first discharge process (lithiation), there is a long discharge plateau between 0 and 0.1 V with Li corresponding to crystalline silicon forming Li_xSi alloy. During the charge process, there is an inclined plateau between 0.4 and 0.5 V, while the Li_xSi alloy changes to Li and amorphous silicon.

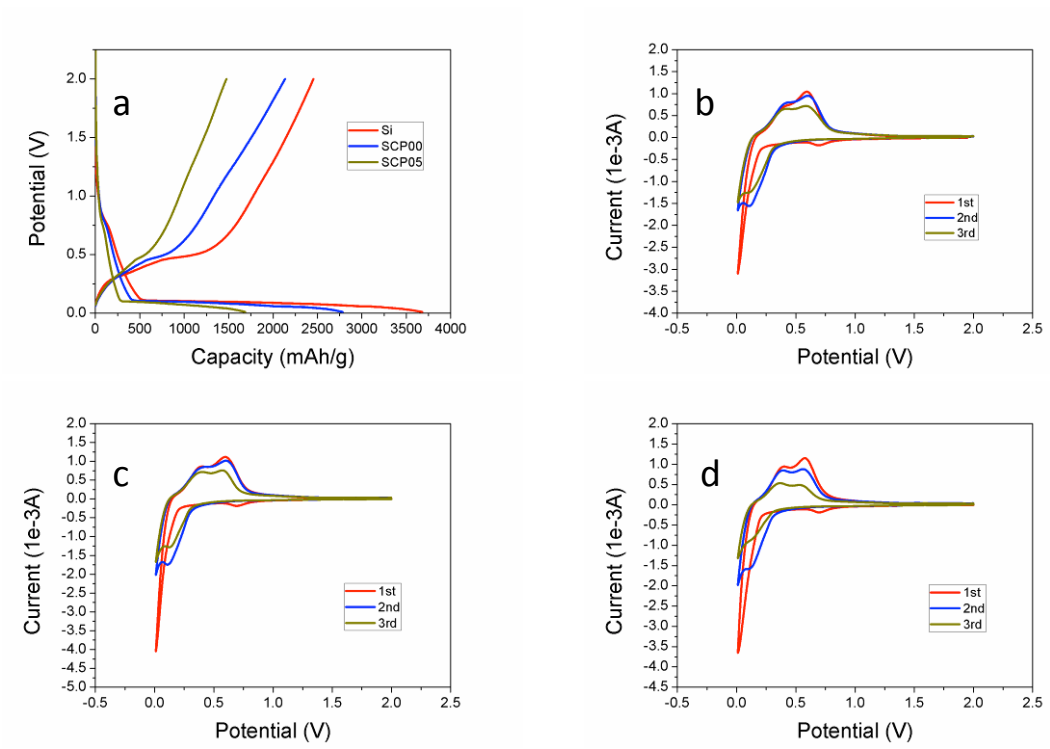

Fig. 5 The initial discharge-charge curves of (a) Si; SCP00; SCP05 and the cyclic voltammograms of (b) Si; (c) SCP00; (d) SCP05.

The cyclic voltammograms of different samples are shown in Fig. 5(b)-(d). The cyclic voltammograms don't exhibit obvious differences after adding CeO_2 and PANI, which means only Si reacts with Li. It's clear that there are two oxidation (delithiation) peaks at 0.37V and 0.55V in anodic curves, and two reduction (lithiation) peaks at 0.01V and 0.12V in cathodic curves. The wide peak between 0.5V and 0.8V in cathodic curve is observed in the first cycle and disappears in the following cycles. It's attributed to the formation of solid electrolyte interface (SEI) film due to the reaction of between composite and electrolyte on the surface of electrode. The crystalline silicon forms alloy with Li in the first cathodic process, and turns to amorphous silicon after delithiation in the first anodic process. In the following cathodic processes, amorphous silicon forms alloy with Li, which are different from

the first one, so the peak at 0.12V doesn't exist in the curve of first cycle [30, 31].

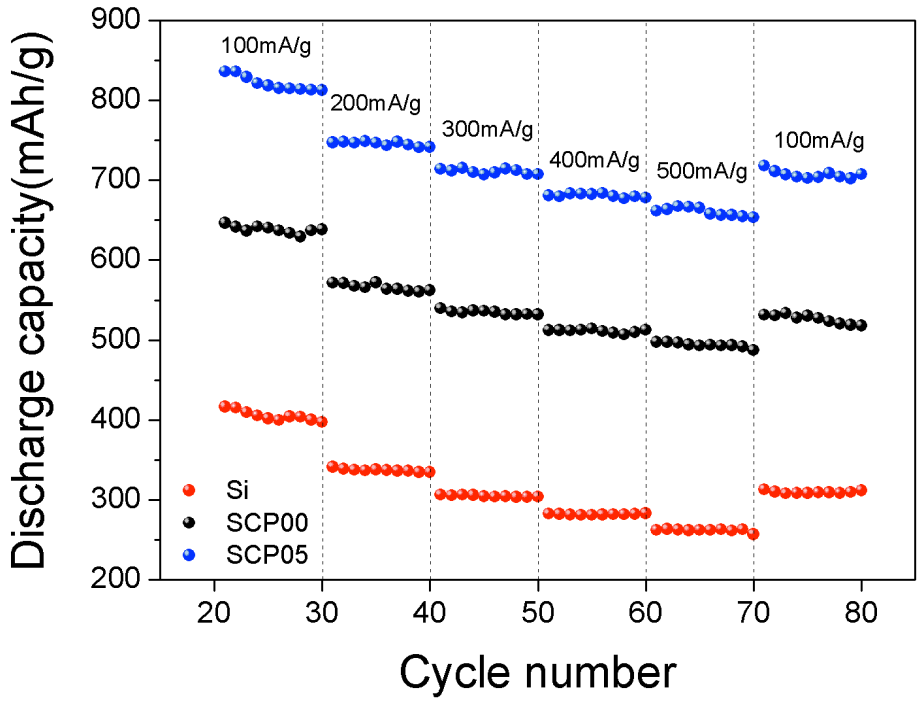

Fig. 6 The cycling performance of Si, SCP00 and SCP05 at different current densities

Fig. 6 shows the cycling performance of samples at different current densities. For the SCP05 electrode, the discharge capacities are 836.3, 747.3, 714.3, 681.2 mAh/g and 661.8 mAh/g at 100, 200, 300, 400 mA/g and 500 mA/g of current densities, respectively; and recovers to 718.2 mAh/g as the current density back to 100 mA/g again. When the current density is decreased again to 100mAh/g, nearly 91.3% of the SCP05's discharge capacity has been retained, while the capacity retention of SCP00 and pure Si are 88.4% and 83.2%. The results demonstrate that SCP05 electrode exhibits better rate performance.

4. Conclusions

The SCP composites have been synthesized through hydrothermal reaction and

chemical polymerization. Some CeO_2 particles distribute on the surface of Si as protective layer. The SCP nanoparticles with an average diameter of 50 nm are well coated by the PANI elastomer with excellent conductivity. The PANI layer of about 3.6nm could be easily recognized and SCP particles are connected with each other by the layer with good elasticity. The SCP05 shows best cycling performance: its initial capacity can reach 1678.6mAh/g with an initial coulombic efficiency of 87.6% and still retains 774.8mAh/g after 100 cycles, 46.2% of the initial capacity kept; while the SCP00 and Si only keep 594.8 and 369.4mAh/g after 100 cycles. The good cycling performance of SCP05 can be attributed to the CeO_2 protecting the SCP material from reacting with the electrolyte. Furthermore, the PANI elastomer can accommodate the volume change of the composite during Li-alloying/dealloying processes, so the pulverization of silicon would be well inhabited.

Acknowledgements

This work is supported by the national 973 project (Contract No. 2009CB220100), the Program for New Century Excellent Talents in University (Contract No. NCET-12-0047 & NCET-13-0033), and Natural Science Foundation of China (Contract No. 21476027).

References

1. Choi, N.-S., et al., *One dimensional Si/Sn - based nanowires and nanotubes for lithium-ion energy storage materials.* Journal of Materials Chemistry, 2011. **21**(27): p. 9825.

2. Chen, M., et al., *Silicon-Graphite-Polyaniline Nanocomposite with Improved Lithium-Storage Capacity and Cyclability as Anode Materials for Lithium-ion Batteries.* International Journal of ELECTROCHEMICAL SCIENCE 2012. **7**: p. 819-829.

3. Yang, S., et al., *Covalent binding of Si nanoparticles to graphene sheets and its influence on lithium storage properties of Si negative electrode.* Journal of Materials Chemistry, 2012. **22**(8): p. 3420.

4. Luo, J., et al., *Crumpled Graphene-Encapsulated Si Nanoparticles for Lithium Ion Battery Anodes.* The Journal of Physical Chemistry Letters, 2012. **3**(13): p. 1824-1829.

5. Tao, H.-C., et al., *Self-supporting Si/Reduced Graphene Oxide nanocomposite films as anode for lithium ion batteries.* Electrochemistry Communications, 2011. **13**(12): p. 1332-1335.

6. Yao, J., et al., *Preparation of Si-PPy-Ag composites and their electrochemical performance as anode for lithium-ion batteries.* Ionics, 2012. **19**(3): p. 401-407.

7. Guzman, R.C., et al., *A silicon nanoparticle/reduced graphene oxide composite anode with excellent nanoparticle dispersion to improve lithium ion battery performance.* Journal of Materials Science, 2013. **48**(14): p. 4823-4833.

8. Wang, B., et al., *Adaptable Silicon–Carbon Nanocables Sandwiched between Reduced Graphene Oxide Sheets as Lithium Ion Battery Anodes.* ACS NANO,

2013. **7**(2): p. 1437-1445.

9. Zhao, G., et al., *Decoration of graphene with silicon nanoparticles by covalent immobilization for use as anodes in high stability lithium ion batteries.* Journal of Power Sources, 2013. **240**: p. 212-218.

10. Lu, D., et al., *Density functional calculations of Lithium-doped few-layer ABA-stacked graphene supported on Pt and Si-terminated SiC surfaces.* Chemical Physics Letters, 2011. **515**(4-6): p. 263-268.

11. Zhu, Y., et al., *Directing silicon-graphene self-assembly as a core/shell anode for high-performance lithium-ion batteries.* Langmuir, 2013. **29**(2): p. 744-9.

12. Zhao, X., et al., *In-Plane Vacancy-Enabled High-Power Si-Graphene Composite Electrode for Lithium-Ion Batteries.* Advanced Energy Materials, 2011. **1**(6): p. 1079-1084.

13. Edfouf, Z., et al., *Nanostructured Ni3.5Sn4 intermetallic compound: An efficient buffering material for Si-containing composite anodes in lithium ion batteries.* Electrochimica Acta, 2013. **89**: p. 365-371.

14. Edfouf, Z., et al., *Nanostructured Si/Sn–Ni/C composite as negative electrode for Li-ion batteries.* Journal of Power Sources, 2011. **196**(10): p. 4762-4768.

15. Liu, Y., et al., *One-pot synthesis of three-dimensional silver-embedded porous silicon micronparticles for lithium-ion batteries.* Journal of Materials Chemistry, 2011. **21**(43): p. 17083.

16. Chen, D., et al., *Reversible lithium-ion storage in silver-treated nanoscale hollow porous silicon particles.* Angew Chem Int Ed Engl, 2012. **51**(10): p.

2409-13.

17. Yu, Y., et al., *Reversible storage of lithium in silver-coated three-dimensional macroporous silicon.* Adv Mater, 2010. **22**(20): p. 2247-50.

18. Wu, X., et al., *Ag-enhanced SEI formation on Si particles for lithium batteries.* Electrochemistry Communications, 2003. **5**(11): p. 935-939.

19. Kwon, E., et al., *Improved rate capability of lithium-ion batteries with Ag nanoparticles deposited onto silicon/carbon composite microspheres as an anode material.* Solid State Ionics, 2013. **237**: p. 28-33.

20. Lu, Z.W., et al., *Electrochemical performance of Si–CeMg12 composites as anode materials for Li-ion batteries.* Journal of Power Sources, 2009. **189**(1): p. 832-836.

21. Chen, Y., et al., *Green synthesis and stable li-storage performance of FeSi(2)/Si@C nanocomposite for lithium-ion batteries.* ACS Appl Mater Interfaces, 2012. **4**(7): p. 3753-8.

22. Li, Y., et al., *Coaxial electrospun Si/C–C core–shell composite nanofibers as binder-free anodes for lithium-ion batteries.* Solid State Ionics, 2014. **258**: p. 67-73.

23. Sim, S., et al., *Critical thickness of SiO2 coating layer on core@shell bulk@nanowire Si anode materials for Li-ion batteries.* Adv Mater, 2013. **25**(32): p. 4498-503.

24. Cheng, H., et al., *Periodic porous silicon thin films with interconnected channels as durable anode materials for lithium ion batteries.* Materials

Chemistry and Physics, 2014. **144**(1-2): p. 25-30.

25. Zhang, Z., et al., *Scalable synthesis of interconnected porous silicon/carbon composites by the rochow reaction as high-performance anodes of lithium ion batteries.* Angew Chem Int Ed Engl, 2014. **53**(20): p. 5165-9.

26. Rong, J., et al., *Coaxial Si/anodic titanium oxide/Si nanotube arrays for lithium-ion battery anodes.* Nano Research, 2013. **6**(3): p. 182-190.

27. Zhao, X., et al., *Growth of Si nanowires in porous carbon with enhanced cycling stability for Li-ion storage.* Journal of Power Sources, 2014. **250**: p. 160-165.

28. Li, H., et al., *Si–Y multi-layer thin films as anode materials of high-capacity lithium-ion batteries.* Journal of Power Sources, 2012. **217**: p. 102-107.

29. Wang, Q., et al., *Synthesis and electrochemical characterizations of Ce doped SnS2 anode materials for rechargeable lithium ion batteries.* Electrochimica Acta, 2013. **93**: p. 120-130.

30. Datta, M.K. and P.N. Kumta, *Silicon, graphite and resin based hard carbon nanocomposite anodes for lithium ion batteries.* Journal of Power Sources, 2007. **165**(1): p. 368-378.

31. Hou, X. H., et al., *The Roles of Intermediate Phases of Li-Si Alloy as Anode Materials for Lithium-Ion Batteries.* Rare Metal Materials and Engineering, 2010. **39**(12): p. 2079-2083.